Modeling Bone Morphogenetic Protein Diffusion of Infuse® Bone Graft

Alicia Lee

Yae Lim Lee

Barnabas Yik

Fall 2012 BENG 221

1. Introduction

Degenerative disc disease (DDD) is when one or more of the intervertebral discs of the spine degenerates. Because of the degenerative changes, the intervertebral disc is unable to accommodate normal biomechanical stresses and may cause compression on nerve roots. This can lead to chronic lower back pain or pain felt when sitting, bending, lifting or twisting, affecting the quality of a person's life [1,3,6].
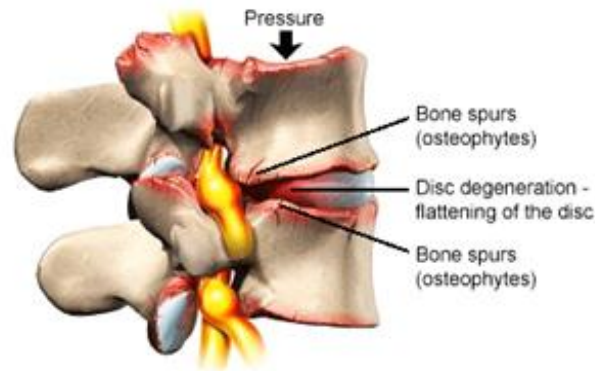

Figure 1 Degenerative Disc Disease

DDD can be treated through non-surgical means through chiropractic treatments such as physical therapy, anti-inflammatory medications, or spinal injections. When these treatments fail to provide pain relief, surgery may be used to treat the disease. Most often spinal fusion is used [1].

Spinal fusion is a surgical technique used to join two or more vertebrae. Although spinal fusion has been used to treat cervical and thoracic problems, it is most commonly done in the lumbar region of the spine. In general, spinal fusion involves taking a bone graft from the patient's pelvis or from a bone bank and implanting the graft between two vertebrae. The bone graft will then simulate bone growth in the area and ultimately fuse the two vertebrae together. The two main types of lumbar spinal fusion are posterolateral fusion and interbody fusion. In posterolateral fusion, the bone graft is placed between the transverse processes in the back of the spine and are fixed in place with screws and/or wires. Interbody fusion places the bone graft between the vertebra in the area usually occupied by the intervertebral disc. There are three different types of lumbar interbody fusion –anterior, posterior and transforaminal. Screws, rods or plates, or cages are used to stabilize the vertebra to facilitate bone fusion [2].

Among the three types, the advantages of anterior lumbar interbody fusion (ALIF) include expanding the disc space and reestablishing normal anatomic alignment and associations of the spinal motion segment without injuring the posterior paravertebral muscles (muscles located behind the spine by the vertebral column). ALIF "also retains posterior stabilizing

structures, avoids epidural scarring and perineural fibrosis and reduces adjacent segment degeneration in the lumbar spine [3]."

In ALIF, the surgeon makes an incision on the lower abdomen to access the spine. Then the surgeon removes the intervertebral disc and replaces it with a bone graft, which is generally taken from the iliac crest (the top rim of the pelvis). Metal hardware can be posteriorly applied to prevent movement between the vertebrae, stabilizing interbody grafts and increasing rates of fusion. If the procedure succeeds, the patient's vertebrae are fused together and full recovery is achieved in about eight months to two years after surgery [3,4,5].
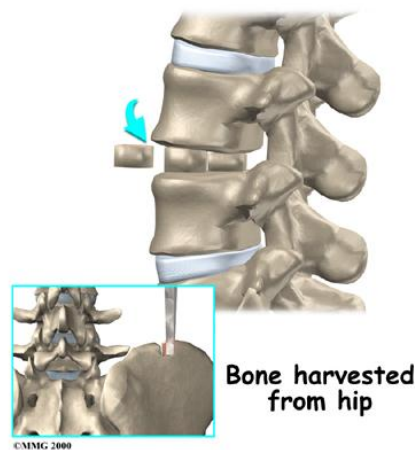

Figure 2 Anterior Lumbar Interbody Fusion

There are many different types of grafts considered for ALIF spine surgery. Allograft bone grafts from cadaveric bone can be used but is generally not as strong as other implants and may lead to further instability. Autografts can be obtained by taking a large bone graft from the patient's iliac crest. This, however, may result in infection or pelvic fracture and is not as strong as allograft bone [8].

Medtronic offers a therapy called The Infuse® Bone Graft/LT-Cage® Lumbar Tapered Fusion Device that eliminates the need to harvest autologous bone graft from the iliac crest [7,9]. The bone graft alternative – Infuse® Bone Graft –consists of a solution containing recombinant human bone morphogenetic protein-2 (rhBMP-2) and an absorbable collagen sponge (ACS) designed to be absorbed over time. Infuse bone graft is placed inside the LT-Cage Lumbar Tapered Fusion Device which restores the degenerated disc space to its original height. Two Infuse® Bone Graft/LT-Cage® Lumbar Tapered Fusion Devices are implanted side by side [9].

Bone morphogenetic protein-2 (BMP-2) is an osteoinductive bone growth factor found in small amounts in the body that stimulates pluripotent cells to form bone. Using recombinant human BMP-2 (rhBMP-2), a genetically engineered version of BMP-2, in interbody fusion cages has shown to be more effective and reliable in treating patients as compared to autogenous bone

graft. The ACS, manufactured from Type I bovine collagen, acts as a scaffold for bone formation that is encouraged by rhBMP-2 [7, 9,10].

After the implantation, mesenchymal stem cells surrounding the tissues infiltrate the implant. RhBMP-2 induces differentiation into osteoblasts that begin to form bone and/or cartilage. Bone formation starts on the outside of the implant, and continues toward the center as the collagen scaffold is adsorbed.

Figure 3 Infuse Bone Graft

2. Problem Statement

A major limitation of clinical BMP-2 injection treatments is its rapid diffusion from the site of implantation. This causes a significant decrease in local concentration as well as rapid loss of bioactivity in the soluble form [18]. It is necessary to obtain a critical density of cells to start the regeneration process [11].

In general, BMP carriers are made to retain BMP/growth factors for a sufficient amount of time to allow cells to migrate into the site of injury and regenerate tissue through proliferation and differentiation. It is also desirable for carriers to be biocompatible and have the ability to be bioresorbable over time, allowing cells to take its place [11].

We would like to model the diffusion of BMP-2 out of the collagen scaffold to determine what the minimum initial concentration needed to maintain an optimum level of BMP-2 in the system for a certain time and distance. It is assumed that there is a minimum concentration of exogenous BMP required to induce a critical density of BMP responsive cells required for effective tissue generation. Therefore, if BMP levels are too low (not retained at a certain level), repair would occur at a slower rate and effective bone formation may not occur as needed.

3. Problem Setup and Assumptions

In this scenario, we modeled the change in BMP concentration using the standard diffusion model and included a concentration-dependent degradation term to more closely mimic real-life setting. We made the assumption that prior to surgery, there is no BMP within the system. Therefore, the concentration of BMP jumps to C0 for the length of the device, which we specified in our initial conditions. To solve this diffusion equation, we require two zero value or flux boundary conditions. Our first boundary conditions come from the fact that no additional BMP is introduced into the system after surgery and we assume that the left end is blocked by the wall of the cage. As a result, flux is set to 0 at the left end of the spine. For our second boundary condition, we make the assumption that the lumbar arteries located near the other end of the spine will uptake the residual BMP that float outside of the spine. Therefore, we have a zero value boundary at the other end of the spine. Finally, to solve this problem analytically, we needed to simplify a few parts of our model. For instance, in real-life, there is a different diffusion coefficient for BMP flowing through the body and BMP flowing through a collagen scaffold. Similarly, there is degradation of BMP in the body, but no degradation in the scaffold. Because we will run into problems determining the positive, negative or zero nature of the eigenvalue, we averaged the coefficients and assumed a single diffusion coefficient and a single degradation coefficient applies for the entire system (See Appendix). The coefficients were averaged based on the ratio of the length of the device to the length of the vertebrae.
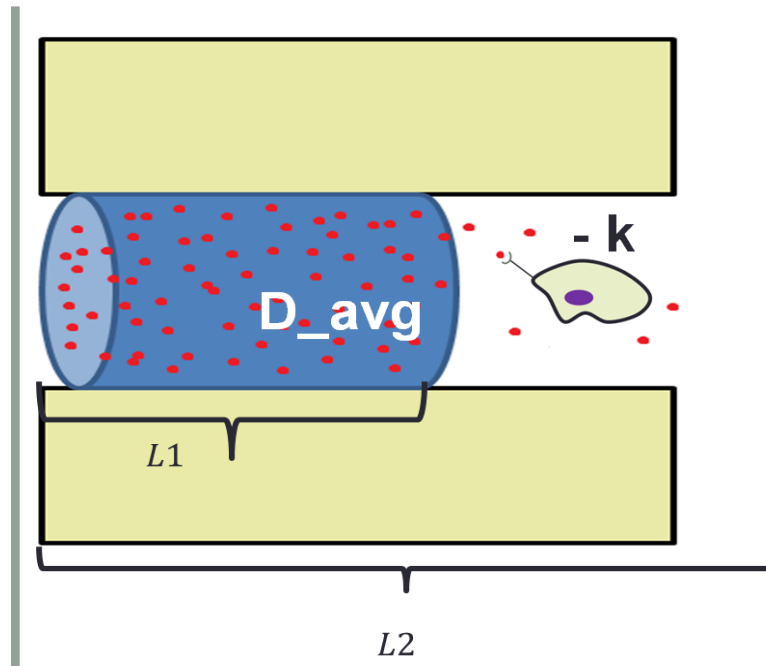

Figure 4 Problem setup with averaged single diffusion coefficient and a single degradation coefficient.

4. Analytical Solution

Our equation: $\frac{\partial C(x,t)}{\partial t} = D \frac{\partial^2 C(x,t)}{\partial x^2} - kC(x,t)$

Boundary condition: $\frac{\partial C}{\partial x}(0,t) = 0$ and $C(L_2,t) = 0$

Initial condition: $g(x) = \begin{cases} C_0 & \text{for } 0 \le x < L_1 \\ 0 & \text{for } L_1 \le x < L_2 \end{cases}$

Coefficients: $D_{avg} = D1\left(\frac{L1}{L2}\right) + D3\frac{(L2-L1)}{L2}$

$$k_{avg} = 0\left(\frac{L1}{L2}\right) + k\frac{(L2-L1)}{L2}$$

Use separation of variables:

$$C(x,t) = \phi(x)G(t)$$

Diffusion equation: $\phi(x)\frac{dG(t)}{dt} = D\frac{d^2\phi(x)}{dx^2}G(t) - k\,\phi(x)G(t)$

Divide every term by $D\,\phi(x)G(t)$: $\frac{\frac{dG(t)}{dt}}{DG(t)} = \frac{\frac{d^2\phi(x)}{dx^2}}{\phi(x)} - \frac{k}{D}$

$$\frac{\frac{dG(t)}{dt}}{DG(t)} + \frac{k}{D} = \frac{\frac{d^2\phi(x)}{dx^2}}{\phi(x)} = -\lambda$$

Time dependent part:

$$\frac{\frac{dG(t)}{dt}}{DG(t)} + \frac{k}{D} = -\lambda$$

$$\frac{dG(t)}{dt} = -\left(\lambda + \frac{k}{D}\right)DG(t)$$

$$G(t) = G_0 e^{-\left(\lambda + \frac{k}{D}\right)Dt}$$

Space dependent part:

$$\frac{\frac{d^2\phi(x)}{dx^2}}{\phi(x)} = -\lambda$$

$$\frac{d^2\phi(x)}{dx^2} = -\lambda\phi(x)$$

Solving for Lambda with Boundary Conditions:

$$\frac{\partial C}{\partial x}(0,t) = 0 \text{ and } C(L_2,t) = 0,$$

(i) $\lambda = 0$: $\phi(x) = Ax + B$

$$A = B = 0 \quad \text{Trivial solution}$$

(ii) $\lambda < 0$: $\phi(x) = Ae^{\sqrt{-\lambda}x} + Be^{-\sqrt{-\lambda}}x$

$$A = B = 0 \quad \text{Trivial solution}$$

(iii) $\lambda > 0$, $\phi(x) = A\cos\left(\sqrt{\lambda}x\right) + B\sin\left(\sqrt{\lambda}x\right)$

$$\text{Since } \frac{\partial C}{\partial x}(0,t) = 0, \quad B = 0$$

$$\text{Since } C(L_2,t) = 0, \quad A\cos\left(\sqrt{\lambda}L_2\right) = 0$$

$$\sqrt{\lambda} = \frac{\left(\frac{1}{2}+n\right)\pi}{L_2} = \frac{(2n+1)}{2}\frac{\pi}{L_2}$$

Resulting eigenmode expansion:

$$C(x,t) = \sum_{n=0}^{\infty} A_n \cos\left(\sqrt{\lambda}x\right) e^{-\left(\lambda+\frac{k}{D}\right)Dt}, \text{ where } \sqrt{\lambda} = \frac{(2n+1)}{2}\frac{\pi}{L_2}$$

Coefficients A_n in the eigenmode expansion satisfy the initial condition:

$$C(x,0) = \sum_{n=0}^{\infty} A_n \cos\left(\sqrt{\lambda}x\right) = g(x) = \begin{cases} C_0 & \text{for } 0 \leq x < L_1 \\ 0 & \text{for } L_1 \leq x < L_2 \end{cases}$$

By orthogonality of the basis function over $[0, L_2]$

$$A_n = \frac{2}{L_2} \int_0^{L_2} g(x)\cos(\sqrt{\lambda}x)dx$$

$$A_n = \frac{2}{L_2} \int_0^{L_1} C_0 \cos\left(\sqrt{\lambda}x\right)dx$$

$$A_n = \frac{4C_0}{(2n+1)\pi} \sin\left(\frac{(2n+1)}{2}\frac{L_1}{L_2}\pi\right), n = 0, 1, 2, 3 \dots$$
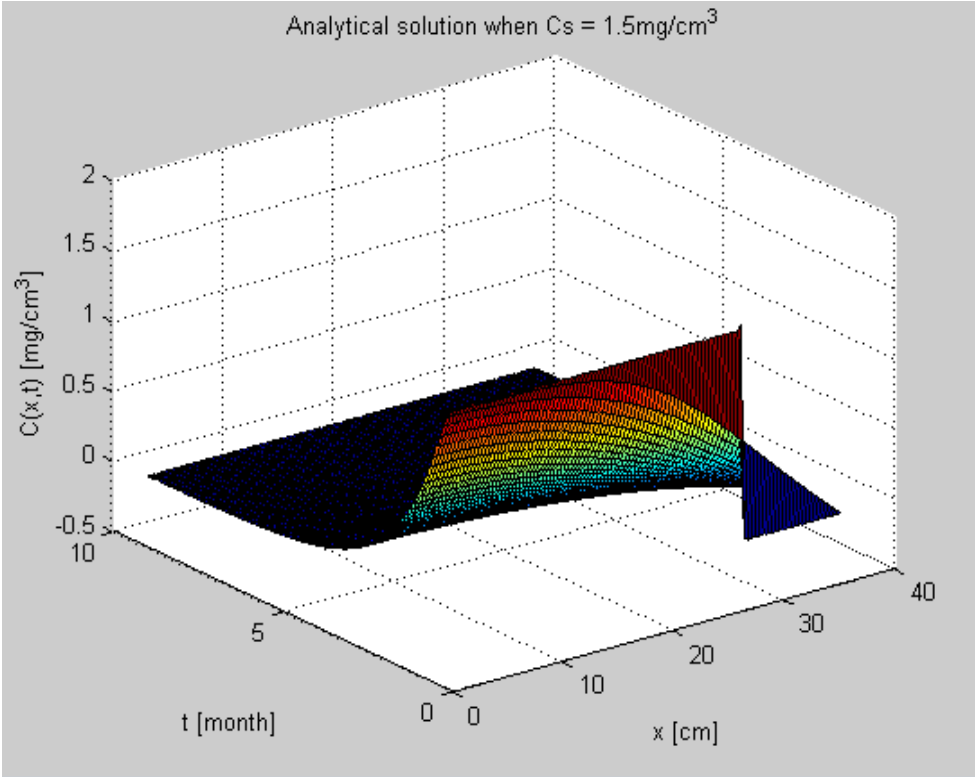
Final solution:

$$C(x,t) = \sum_{n=0}^{\infty} A_n \cos\left(\sqrt{\lambda}x\right) e^{-\left(\lambda+\frac{k}{D}\right)Dt}, \text{ where } \sqrt{\lambda} = \frac{(2n+1)}{2}\frac{\pi}{L_2}$$

$$A_n = \frac{4C_0}{(2n+1)\pi} \sin\left(\frac{(2n+1)}{2}\frac{L_1}{L_2}\pi\right), n = 0,1,2,3 \dots$$

Parameter	Value	Source
Estimated diffusion of BMP in body	1×10^{-6} cm2/s	16
Estimated diffusion of BMP in collagen	Dcollagen is about 10 times faster than Dbody	17
Diffusion of BMP with fibrin glue	In vitro rh-BMP2 release is 2 times faster without fibrin glue.	20
Degradation Rate of BMP	These cells release 20-125 ng/ml of BMP-2 into 7-8 ml of supernatant in 48 h, i.e., ≈3-20ng/hr.Rates were ≈0.06-0.12 ng/hr for both cell types. Estimated BMP-2 degradation as 1% of production rate	12
Length of vertebrae	≈32- 35mm	14,19
Length of cage	The cage has a tapered design with an angle of 8.8° and is available in diameters ranging from 14mm to 18mm at the narrow end of the taper, 17mm to 22mm at the wide end of the taper and in lengths ranging from 20mm to 26mm.	15
Length of time	I was told it takes at least 3 months to see any real bone growth… Today, 9 months after his spinal surgery, Josh says he's "pretty close to normal."	21
Initial source concentration	1.5mg/mL	22
Minimum Concentration required for bone growth	0.032mg/mL	20

Table 1 Values for the parameters found in literature

Surface plot of analytical solution approximated using the first 500 terms of the series were plotted in Figure 5. Parameter values defined in Table 1 were used. Upper plot of Figure 5 shows that our analytical solution satisfies the initial condition successfully. Concentration of BMP decreases continuously from the source to the end where blood vessel is located as expected.
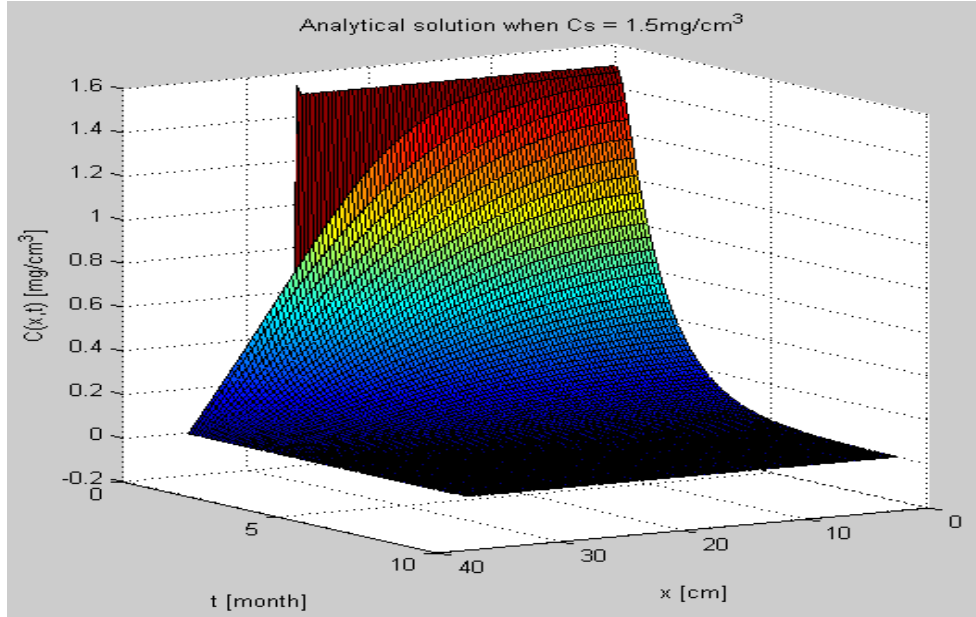
Figure 5 Surface plot of analytical solution using parameter values defined in Table 1. Two rotated view are plotted above

To investigate the optimal initial source concentration to maintain the minimum concentration required for the bone growth throughout the treatment time, the analytical solution of the concentration was plotted with varying initial source concentrations. Since the typical treatment time is nine months, concentration over space was plotted at t = 9 month [Figure 6]. Currently clinicians are using 1.5 mg/cm^3, so we tried the lower and higher values, 0.7 and 1.8 mg/cm^3. For the proper bone growth, we want to maintain concentration above C_{min} = 0.03 mg/cm^3 up to x = 31cm [Table 1]. However, concentration calculated by our analytical solution is too small for the required C_{min}, as can be seen in Figure 6. This result indicates that our analytical solution has a problem with predicting the accurate concentration over time, because initial source concentration of 1.5 mg/cm^3 is successfully used by clinicians. The accuracy of our analytical solution was limited by the one section model where we assumed a single diffusion coefficient and a single degradation coefficient. Therefore, for more accurate analysis, we need to model two section system using MATLAB (See Appendix).
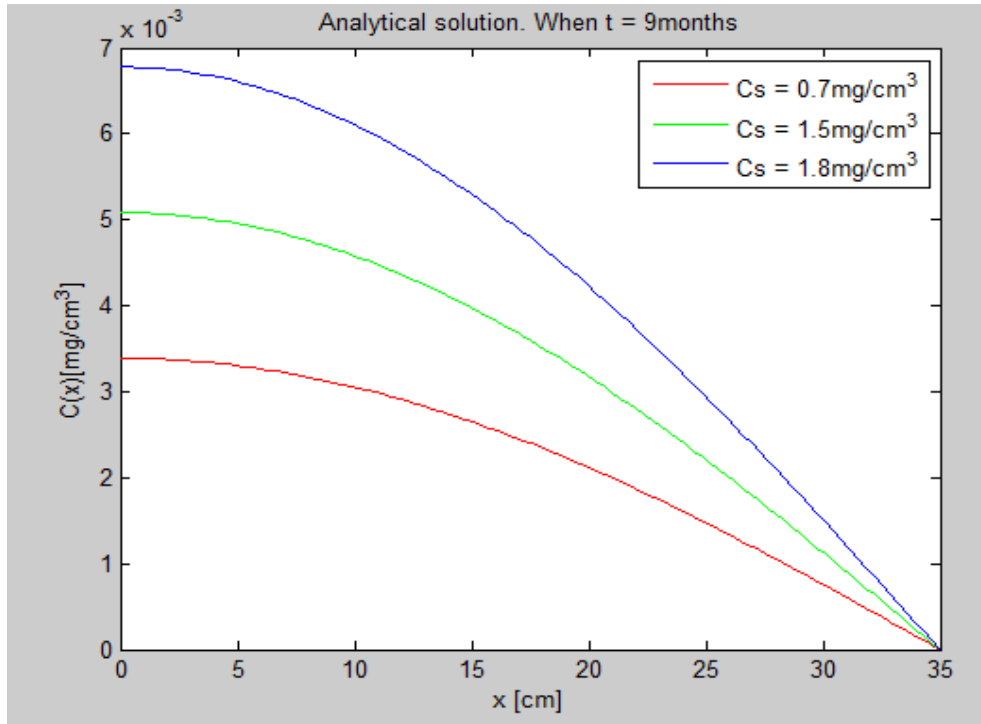
11

Figure 6 Concentration over space of analytical solution after nine months of treatment. Initial source concentrations were varied as 0.7, 1.5, and 1.8 mg/cm^3.

5. Numerical Solution

5-1. One section model

Surface plot of one section model was plotted in Figure 7. Concentration over space of one section model varying initial source concentrations was also plotted in Figure 8. Both plots were consistent with the analytical solution plotted in Figures 5 and 6.
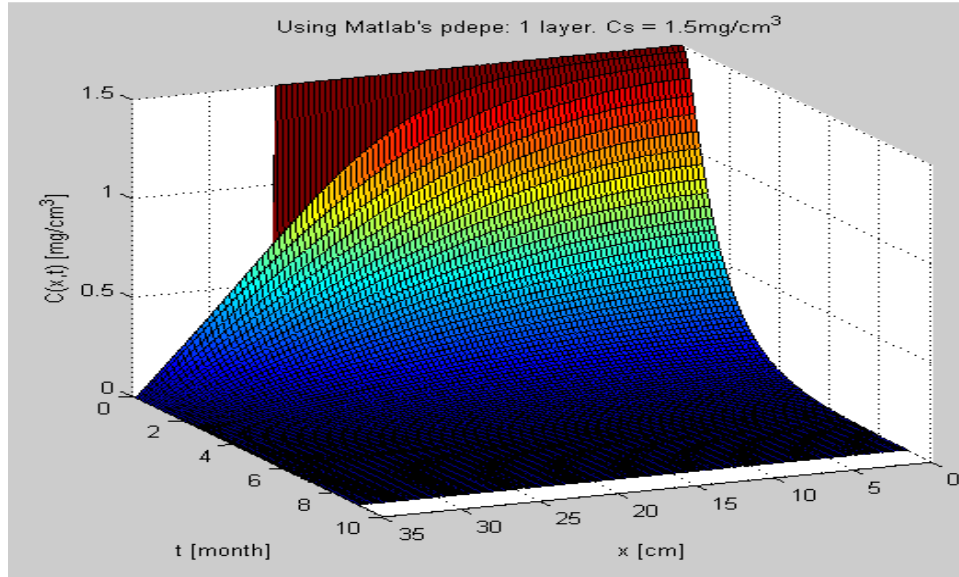
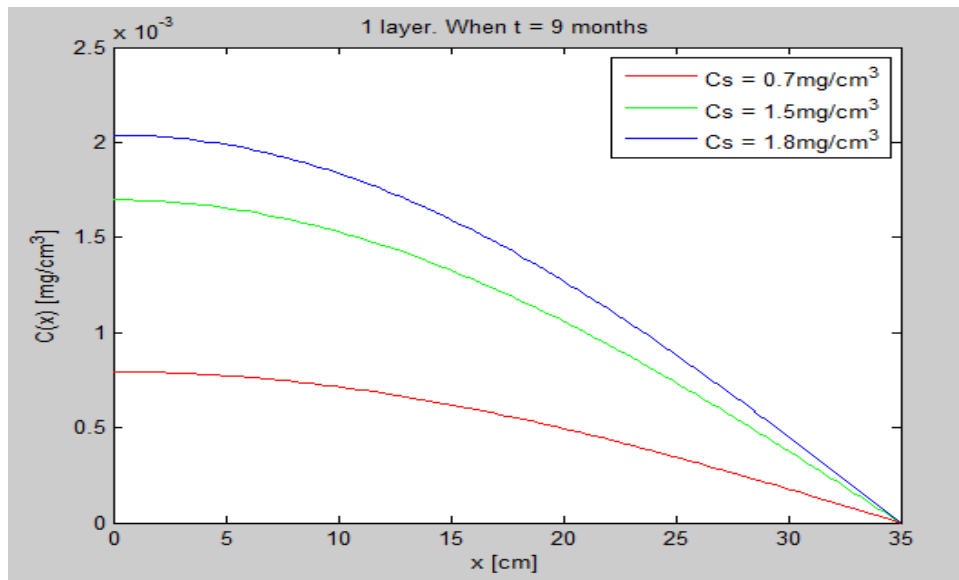**Figure 7** Surface plot of numerical solution of one section model

Figure 8 Concentration over space of numerical solution of one section model after nine months of treatment. Initial source concentrations were varied as 0.7, 1.5, and 1.8 mg/cm^3.

5-2. Two section model

As discussed in Section 4, the one section model could not accurately simulate the concentration of BMP over time. Therefore, we implemented a two section model using the PDEPE function of MATLAB. In the two section model, the collagen scaffold (x = 0 to L1) and the body (x = L1 to L2) have different diffusion coefficients D1 and D3, and there is no

degradation within the collagen scaffold. BMP is degraded linearly in the body with the degradation term –k [Figure 9].
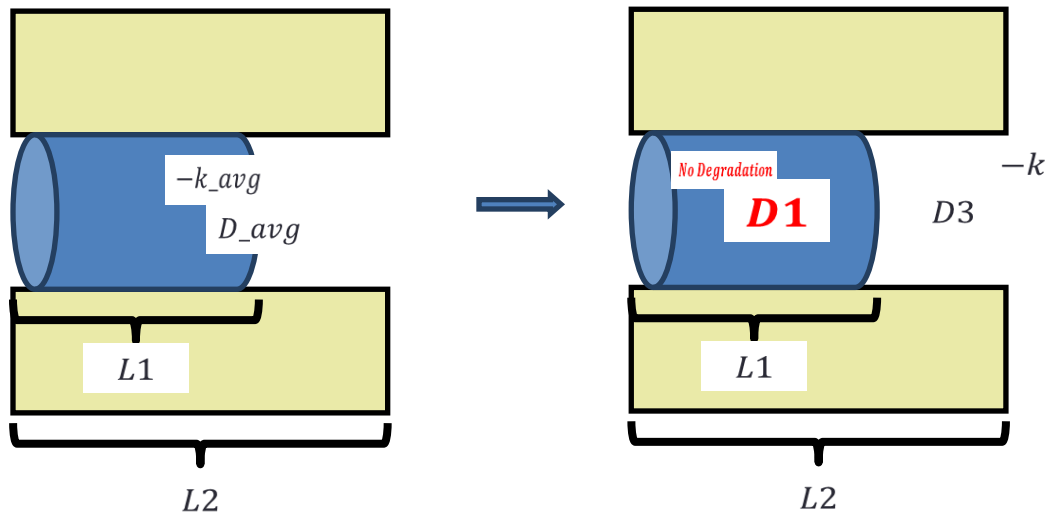

Figure 9 Problem setup: transition from one section model to two section model
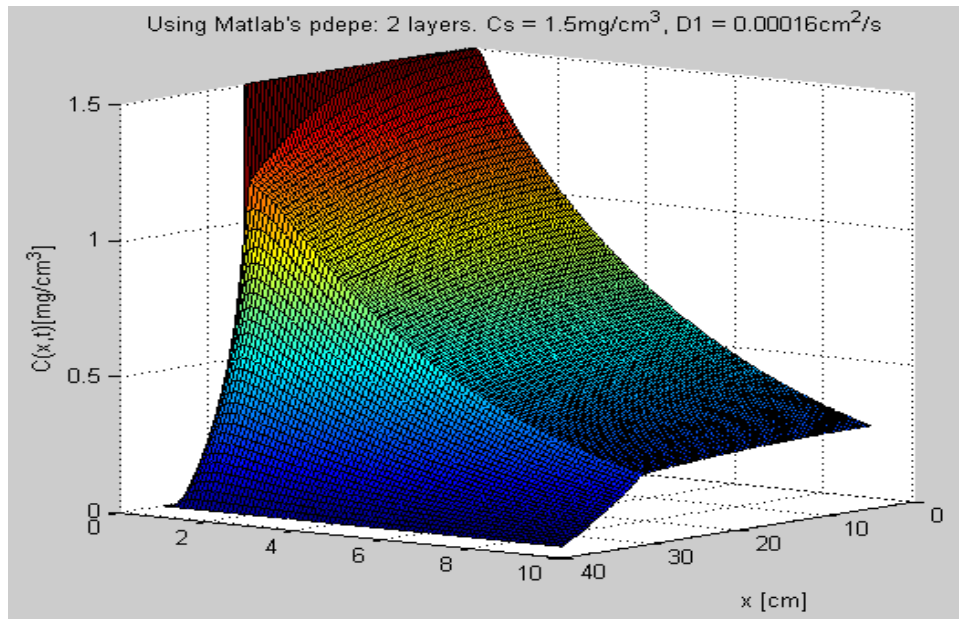

Figure 10 Surface plot of numerical solution of two section model

Surface plot of two section model is plotted in Figure 10. Compared to the surface plot of one section model in Figures 5 and 7, we could observe the abrupt change between section 1 and section 2. Since there is no degradation in section 1, the concentration decreases slowly. As in the one section model, numerical solution of two section model was plotted by varying the initial source concentration to investigate the optimal initial source concentration to maintain the

minimum concentration required for the bone growth throughout the treatment time [Figure 11]. After the typical treatment time, 9 months, the simulated level of BMP was indeed maintained above $C_{min} = 0.03$ mg/cm^3 up to x = 30cm, as expected from the clinical data. This result shows that two section model is simulating the concentration of BMP more accurately than one section model. When $C_{source} = 1.5$ mg/cm^3, which is the value that clinicians are currently using, the concentration at x = 30cm after nine months was about 0.09 mg/cm^3. When we decreased the initial concentration to 0.7 mg/cm^3, the concentration at x = 30cm after nine months was about 0.04 mg/cm^3, which was close to C_{min}. Therefore, according to the two section model, the minimum initial source concentration that clinicians are allowed to use is about 0.7 mg/cm^3. We also tried out initial source concentration larger than the currently using value. When $C_{source} = 1.8$ mg/cm^3, the concentration of BMP over space increased as expected. This model would be helpful to clinicians who would like to investigate how to control the concentration of BMP over time to match the patients' needs.
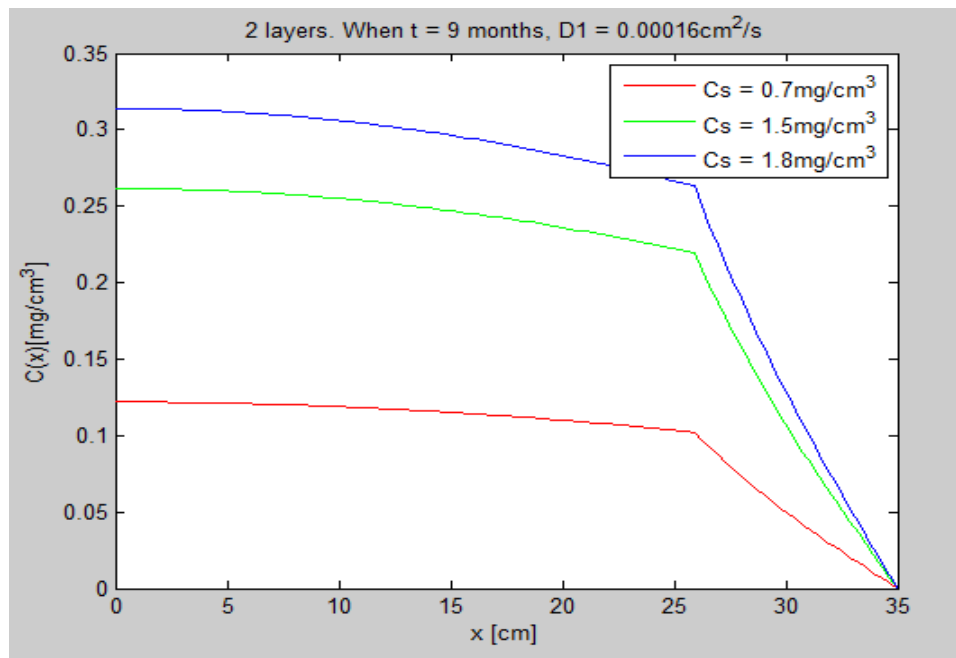

Figure 11 Concentration over space of numerical solution of two section model after nine months of treatment. Initial source concentrations were varied as 0.7, 1.5, and 1.8 mg/cm^3.

To investigate how the diffusion coefficient of the scaffold affects the concentration of BMP over space and time, we simulated the two section model varying the diffusion coefficient. Although collagen is used as a scaffold currently, we could vary the diffusion coefficient of the scaffold by changing the porosity or even the material of the scaffold. Diffusion coefficient of the current scaffold is 1.6×10^{-5} cm^2/sec, and we varied the value from 8×10^{-5} cm^2/sec to 2.4×10^{-5} cm^2/sec. Concentration over space after typical treatment time, 9 month, was plotted in Figure

15

12, but there was no significant difference between models with different diffusion coefficient of the scaffold. Concentration over time at x = 32cm was plotted in Figure 13, and there was a significant difference between models with different diffusion coefficient of the scaffold from 3 weeks to 10 weeks. Therefore, variation of the diffusion coefficient of scaffold affects the concentration of BMP at initial period of the treatment time. Therefore, from the two section model simulation, we found out that diffusion coefficient of the scaffold can be tweaked if clinicians need to change and control the BMP concentration at the early period of the treatment to maximize bone growth.
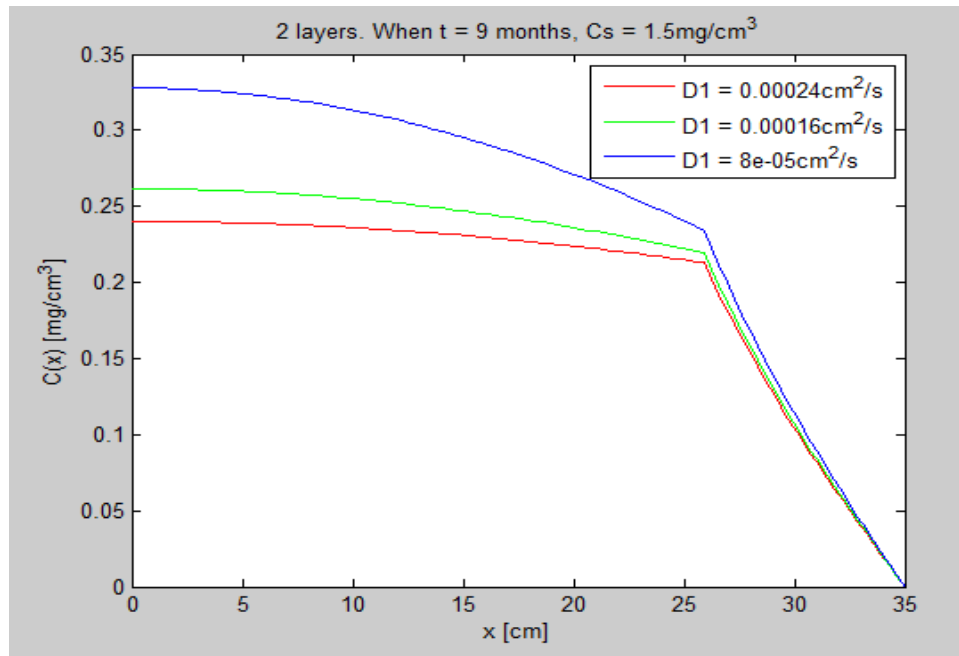

Figure 12 Concentration over space of numerical solution of two section model after nine months of treatment. Diffusion coefficient of the scaffold was varied as 8x10^{-5}, 1.6x10^{-5}, and 2.4 x10^{-5}, cm^2/sec

Figure 13 Concentration over time of numerical solution of two section model at x = 31.15cm. Diffusion coefficient of the scaffold was varied as 8×10^{-5}, 1.6×10^{-5}, and 2.4×10^{-5} cm^2/sec

5-3. Three section model
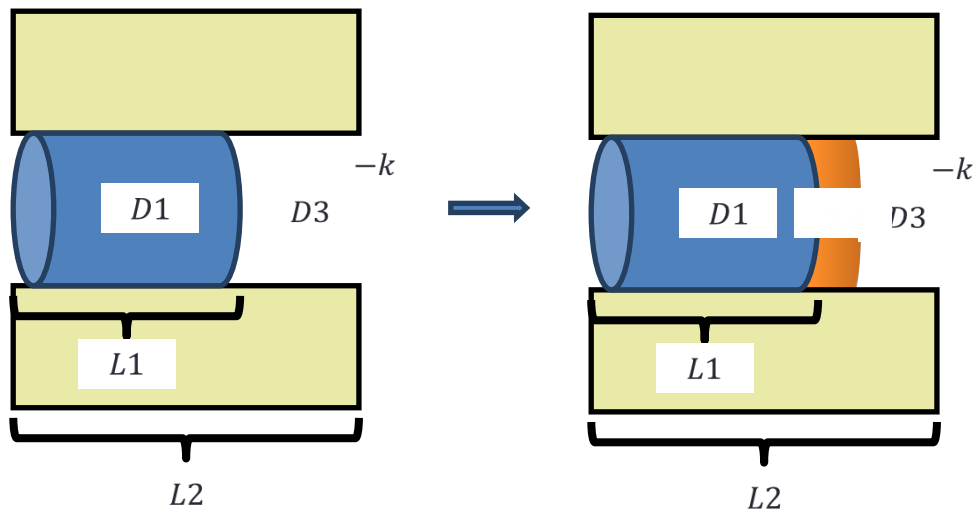
Figure 14 Problem setup: transition from two section model to three section model

While we were studying the literature to develop our project, we found that scientists are recently adding another section with fibrin glue at the end of the scaffold to control the diffusion

of BMP more precisely. A three section device is not currently used clinically, but it is highly likely to be used in the future. It would be meaningful to simulate how this newly added section affects the concentration of BMP through MATLAB modeling. In this section, a three section model was built, simulated, and analyzed. As shown in Figure 14, in our three section model, the first section (scaffold) has a diffusion coefficient D1, the second section (fibrin glue) has a diffusion coefficient D2, and the third section (body) has a diffusion coefficient D1. Degradation is only in the third section (body) with degradation term –k.

The surface plot of the numerical solution of three section model is plotted in Figure 15. Three sections are still distinguishable in the plot. Concentration over space after typical treatment time, 9 months, was also plotted with varying the initial source concentration [Figure 16]. The two plots of the three section model are very similar to those of two section model. This is most likely because the length of the fibrin glue is very short, and the values for D1 and D2 are similar.
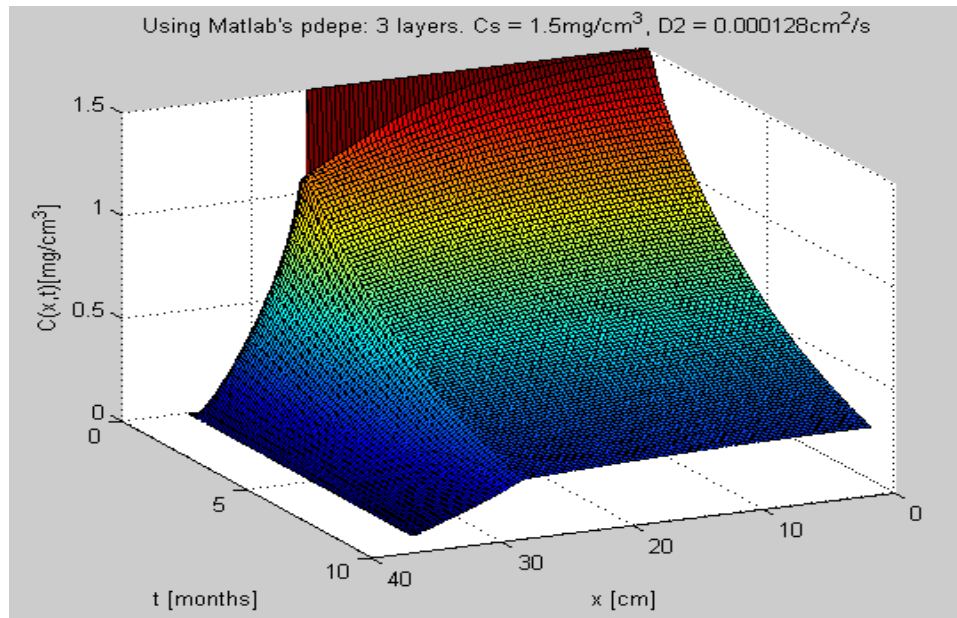
Figure 15 Surface plot of numerical solution of three section model

To closely investigate how the diffusion coefficient of the fibrin glue affects the concentration of BMP over space and time, we simulated the three section model varying the diffusion coefficient of the fibrin glue. Diffusion coefficient of the current fibrin glue section is 12.8×10^{-5} cm^2/sec, and we varied the value from 4.8×10^{-5} cm^2/sec to 19.2×10^{-5} cm^2/sec. Concentration over space after typical treatment time, 9 months, was plotted in Figure 17, and concentration over time at x = 32cm was plotted in Figure 18. Again, there is no significant difference between models with different diffusion coefficients of the fibrin glue, because the fibrin glue section is too thin. Although there is no significant impact of a fibrin glue section in

the simulated results using the current parameters, the three section model provides more accurate and precise model that clinicians can use. If the parameters, such as length and the diffusion coefficient of the fibrin glue section, changes in the future, this three section model would be more useful.
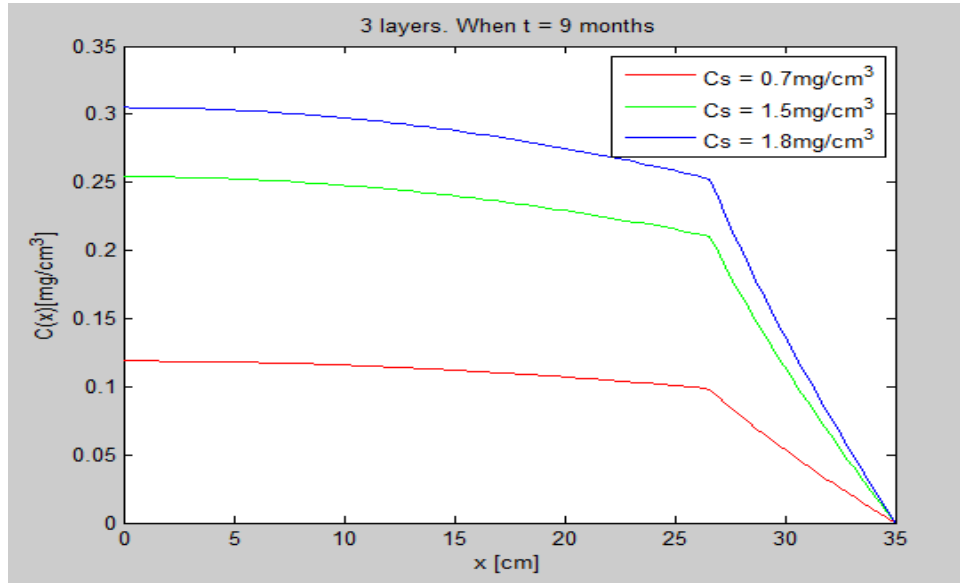
Figure 16 Concentration over space of numerical solution of three section model after nine months of treatment. Initial source concentrations were varied as 0.7, 1.5, and 1.8 mg/cm^3.

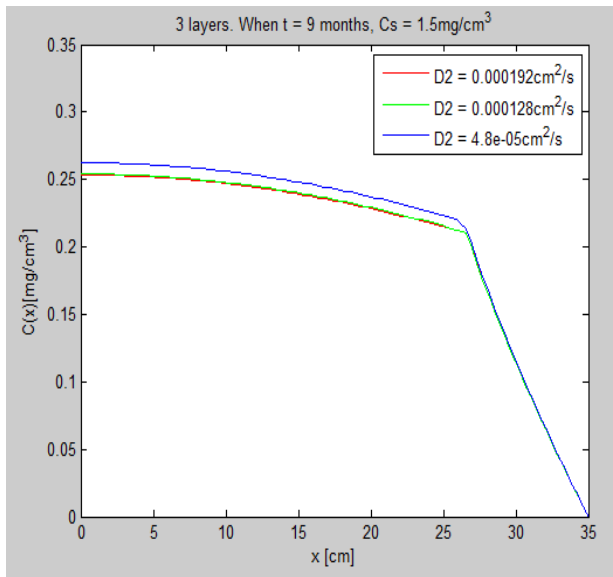**Figure 17** Concentration over space of numerical solution of two section model after nine months of treatment. Diffusion coefficient of the fibrin glue was varied as 4.8, 12.8, and 19.2x10^{-5}cm^2/sec
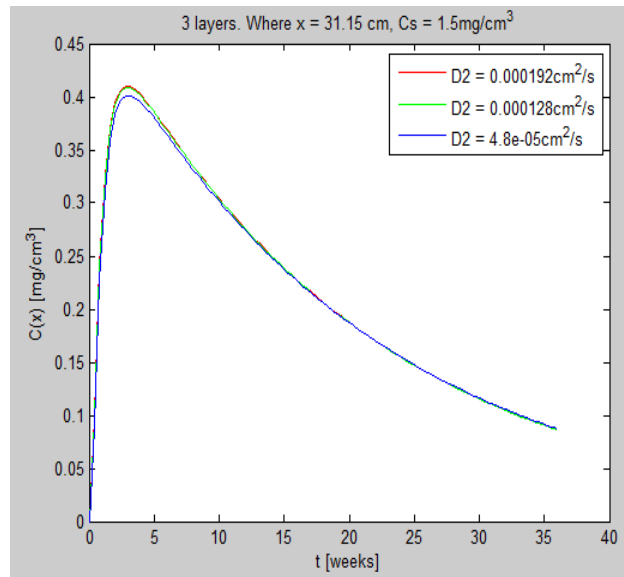
Figure 18 Concentration over time of numerical solution of two section model at x = 31.15cm. Diffusion coefficient of the fibrin glue was varied as 4.8x10^{-5}, 12.8x10^{-5}, and 19.2x10^{-5} cm^2/sec

Future Work

      Although this model provides a good elementary model for making estimates in the initial concentration, modeling the diffusion of BMP-2 in three dimensions would provide a more accurate tool for physicians. In a real-life setting, the diffusion of BMP occurs in the x,y and z directions and the rate of diffusion in each of these directions is affected by the size and shape of the opening in the lumbar cage. For instance, the opening of the cage in the x-direction will have a different effect on diffusion than the two smaller circular openings in the y-direction. Another issue that this 3 dimension model would have to take into account is the anatomical shape and environment of the spine. BMP traveling in the y-direction may encounter blood vessels or other constructs faster than BMP traveling in the x-direction so these additional factors will need to be taken into account. However, this more detailed version of the model would help account for some of the odd factors in our results. For instance, the level of BMP within the scaffold decreased to roughly 20% after 9 months. While this is plausible, it is still concerning that so much BMP still remains in the scaffold at the end of the treatment. However, if you consider that BMP is actually flowing in various directions, the amount of BMP leaving the scaffold should actually be much higher than what we modeled in this one-directional system. Finally, our model would be better if there was more accurate data on the diffusion coefficients of BMP in different environments so we would not have to extrapolate values for our coefficients. Nevertheless, this model is a first step towards a successful modeling of the Infuse Bone Graft Device and may still provide relevant information for physicians when they consider what concentration of BMP to use.

References

[1] "Degenerative disc disease." *Wikipedia: The Free Encyclopedia*. Wikimedia Foundation, Inc. 9 October 2012. Web. 25 Oct. 2012. < http://en.wikipedia.org/wiki/Degenerative_disc_disease>

[2] "Spinal Fusion." *Wikipedia: The Free Encyclopedia*. Wikimedia Foundation, Inc. 3 September 2012. Web. 25 Oct. 2012. < http://en.wikipedia.org/wiki/Degenerative_disc_disease>

[3] Burkus JK, Gornet MF, Dickman CA, Zdeblick TA. "Anterior Lumbar Interbody Fusion Using rhBMP-2 With Tapered Interbody Cages." *Journal of Spinal Disorders & Techniques* Vol. 15, No. 5, pp. 337–349 <http://webdoc.nyumc.org/nyulmc-rehab/files/nyulmc-rehab/u19/bmppivotalstudy.pdf>

[4] "Anterior Lumbar Interbody Fusion." *eORTHOPOD®* . 2011.   Medical Multimedia Group, L.L.C. . 25 Oct 2012. <http://www.eorthopod.com/content/anterior-lumbar-interbody-fusion>.

[5] Flynn JC, Hoque MA. "Anterior fusion of the lumbar spine: End-result study with long-term follow-up." *J Bone Joint Surg Am,* 1979 Dec 01;61(8):1143-1150

[6] "Anterior Lumbar Interbody Fusion." *Lumbar Spine/Lower Back*. 2011.   University Spine Associates, P.A.. 25 Oct 2012. <http://www.universityspine.com/anterior-lumbar-interbody-fusion.html>.

[7] Boden SD, Zdeblick TA, Sandhu HS, Heim SE. "The Use of rhBMP-2 in Interbody Fusion Cages." *SPINE*.Vol. 25(3), 1 February 2000, pp 376-381.< http://www.mendeley.com/research/rhbmp-2-interbody-fusion-cages-definitive-evidence-osteoinduction-humans-preliminary-report/>

[8] Ullrich, PF Jr. "Anterior Lumbar Interbody Fusion Spinal Implants and Bone Grafts." *Spine-Health* . 21 Dec. 2009.   Spine-Health . 25 Oct 2012. <http://www.spine-health.com/treatment/back-surgery/anterior-lumbar-interbody-fusion-spinal-implants-and-bone-grafts>.

 [9] "About Spinal Fusion." *Spinal Fusion*. 22 Sep 2010.   Medtronic, Inc. . 25 Oct 2012. <http://www.medtronic.com/for-healthcare-professionals/products-therapies/spinal-orthopedics/therapies/spinal-fusion/index.htm>.

[10] "How INFUSE® Bone Graft Works." *INFUSE® Bone Graft/LT-Cage® Device*. 29 Sept 2006.   Medtronic   Sofamor   Danek.   25   Oct   2012. <https://www.infusebonegraft.com/how_infuse_works.html>.

[11] Seeherman H, Wozney JM. "Delivery of bone morphogenetic proteins for orthopedic tissue regeneration." *Cytokine Growth Factor Rev*. 16 (2005), pp. 329–345. <http://www.sciencedirect.com/science/article/pii/S1359610105000572>.

[12] Garfinkel A, Tintut Y, Petrasek D, Boström K, Demer L. "Pattern formation by vascular mesenchymal cells." *Proc Natl Acad Sci USA*. 2004 Jun 22;101(25):9247-50. Epub 2004 Jun 14. <http://www.ncbi.nlm.nih.gov/pmc/articles/PMC438961/>

[13] Patel VV, Zhao L, Wong P, Kanim L, Bae HW, Pradhan BB, Delamarter RB. "Controlling bone morphogenetic protein diffusion and bone morphogenetic protein-stimulated bone growth using fibrin glue." *Spine (Phila Pa 1976)*. 2006 May 15;31(11):1201-6. <http://www.ncbi.nlm.nih.gov/pubmed/16688032>

[14] Tan SH, Teo EC, Chua HC. "Quantitative three-dimensional anatomy of lumbar vertebrae in Singaporean Asians." *Eur Spine J*. 2002 Apr;11(2):152-8. Epub 2001 Nov 27. <http://www.ncbi.nlm.nih.gov/pubmed/11956922>

[15] Infuse FDA Approval letter. Available at: http://www.fda.gov/cdrh/mda/docs/p000058.html Accessed Oct 25, 2012

[16] "Diffusion – useful equations." Life Sciences. University of Illinois at Urbana-Champaign. 25 Oct 2012. <http://www.life.illinois.edu/crofts/bioph354/diffusion1.html>.

[17] Wallace DG, Rosenblatt J. "Collagen gel systems for sustained delivery and tissue engineering." *Adv Drug Deliv Rev*. 2003 Nov 28;55(12):1631-49.< http://www.ncbi.nlm.nih.gov/pubmed/14623405>

[18] Doctoral Thesis / Dissertation, 2010 <http://www.grin.com/en/doc/237946/delivery-of-bmp-2-for-bone-tissue-engineering-applications>

[19] Vega EU, Elizondo Omaña RE, Castro O, Lopez SG. "Morphometry of Pedicle and Vertebral Body in a Mexican Population by CT and Fluroscopy." *Int. J. Morphol*. 27(4):1299-1303, 2009.

[20] Patel VV, Zhao L, Wong P, et al. "An in vitro and in vivo analysis of fibrin glue use to control bone morphogenetic protein diffusion and bone morphogenetic protein–stimulated bone growth." *Spine J*. 2006 Jul-Aug. 6(4):397-403.

[21] "Josh's Story." Medtronic. 25 Oct 2012 <http://www.medtronic.com/patients/lumbar-degenerative-disc-disease/personal-stories/josh/index.htm>

[22] McKay WF, Peckham SM, Badura JM. "A comprehensive clinical review of recombinant human bone morphogenetic protein-2 (INFUSE Bone Graft)." *Int Orthop*. 2007 Dec;31(6):729-34. Epub 2007 Jul 17.

Appendix A: Analytical method to solve 2 section model

If we wanted to take into account the different diffusion and degradation coefficients in the system, we would need to split the system into two parts. In system 1, the diffusion coefficient for BMP through collagen would be D1 and there would be no degradation. In the other system, the diffusion coefficient for BMP in the body would be D3 and there would be a degradation coefficient of k. In this two section system, we would need to redefine our boundary conditions such that the right boundaries of the first system has equal flux and value to the left boundary conditions in our second system.
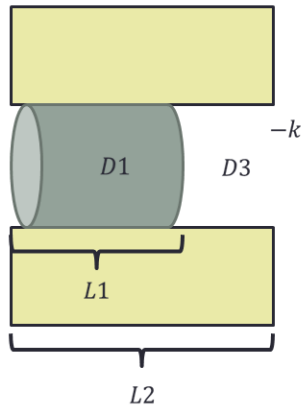
- System 1:
  - $\frac{\partial C_1(x,t)}{\partial t} = D \frac{\partial^2 C_1(x,t)}{\partial x^2}$

- Boundary condition:
  - $\frac{\partial C_1}{\partial x}(0,t) = 0$
  - $C_1(L_1,t) = C_2(L_1,t)$
  - $\frac{\partial C_1}{\partial x}(L_1,t) = \frac{\partial C_2}{\partial x}(L_1,t)$

- Initial condition:
  - $g(x) = C_0$

- System 2:
  - $\frac{\partial C_2(x,t)}{\partial t} = D \frac{\partial^2 C_2(x,t)}{\partial x^2} - k\, C_2$

- Boundary condition:
  - $C_1(L_1,t) = C_2(L_1,t)$
  - $\frac{\partial C_1}{\partial x}(L_1,t) = \frac{\partial C_2}{\partial x}(L_1,t)$
  - $C_2(L_2,t) = 0$

- Initial condition:
  - $g(x) = 0$

When we try to solve it analytically by solving for the identity of lambda, we discover that we have multiple possible solutions that could satisfy our new boundary condition scenarios.

- System 1:
  - $\frac{\partial C_1(x,t)}{\partial t} = D \frac{\partial^2 C_1(x,t)}{\partial x^2}$

- Boundary condition:
  - $\frac{\partial C_1}{\partial x}(0,t) = 0$
  - $C_1(L_1,t) = C_2(L_1,t)$
  - $\frac{\partial C_1}{\partial x}(L_1,t) = \frac{\partial C_2}{\partial x}(L_1,t)$

- Initial condition:
  - $g(x) = C_0$

- (i) $\lambda = 0: \phi(x) = A_1 x + B_1$
  - $\frac{\partial C_1}{\partial x}(0,t) = 0;\ A_1 = 0$
  - $C_1(L_1,t) = C_2(L_1,t);\ B_1 = C_2(L_1,t)$
  - Possible solution?

- (ii) $\lambda < 0: \phi(x) = A_1 e^{\sqrt{-\lambda}x} + B_1 e^{-\sqrt{-\lambda}x}$
  - $\frac{\partial C_1}{\partial x}(0,t) = 0$
  - $A_1 = B_1 = 0$ Trivial solution

- (iii) $\lambda > 0, \phi(x) = A_1 \cos\left(\sqrt{\lambda}x\right) + B_1 \sin\left(\sqrt{\lambda}x\right)$
  - $\frac{\partial C_1}{\partial x}(0,t) = 0;\ B_1 = 0$
  - $C_1(L_1,t) = C_2(L_1,t);$
  - $A_1 \cos\left(\sqrt{\lambda} * L_1\right) = C_2(L_1,t)$
  - Possible Solution?

23

- **System 2:**
  - $\frac{\partial C_2(x,t)}{\partial t} = D \frac{\partial^2 C_2(x,t)}{\partial x^2} - k\, C_2$

- **Boundary condition:**
  - $C_1(L_1, t) = C_2(L_1, t)$
  - $\frac{\partial C_1}{\partial x}(L_1, t) = \frac{\partial C_2}{\partial x}(L_1, t)$
  - $C_2(L_2, t) = 0$

- **Initial condition:**
  - $g(x) = 0$

- (i) $\lambda = 0$: $\phi(x) = A_2 x + B_2$
  - $C_2(L_2, t) = 0$; $A_2(L_2) + B_2 = 0$
  - $\frac{\partial C_2}{\partial x}(L_1, t) = \frac{\partial C_2}{\partial x}(L_1, t)$
  - $C_1(L_1, t) = C_2(L_1, t)$;
  - Possible solution?

- (ii) $\lambda < 0$: $\phi(x) = A_2 e^{\sqrt{-\lambda}x} + B_2 e^{-\sqrt{-\lambda}x}$
  - $\frac{\partial C_1}{\partial x}(0, t) = 0$
  - $A_2 = B_2 = 0$ Trivial solution

- (iii) $\lambda > 0$, $\phi(x) = A_2 \cos\left(\sqrt{\lambda}x\right) + B_2 \sin\left(\sqrt{\lambda}x\right)$
  - $C_2(L_2, t) = 0$; $A_2 \cos\left(\sqrt{\lambda} * L_2\right) + B_2 \sin\left(\sqrt{\lambda} * L_2\right) = 0$
  - $\frac{\partial C_2}{\partial x}(L_1, t) = \frac{\partial C_2}{\partial x}(L_1, t)$
  - $C_1(L_1, t) = C_2(L_1, t)$;
  - Possible solution?

As a result, we chose to solve this system numerically with MATLAB's pdepe.

Appendix B: MATLAB code

```
%% Beng 221 Team Project

function Project()
    clear
    clc
    close all

    %% Defining the variables
    global D1
    global D2
    global D3
    global D_avg
    global k_avg
    global k
    global L_1
    global L_2
    global L_f
    global Cs
```

```matlab
    L_f = 35;                               %[cm]
    L_2 = 26.5;                             %[cm]
    L_1 = 26;                               %[cm]

    D3 = 1.6e-5;                            %[cm^2/s]
    D1_list = [15*D3, 10*D3, 5*D3];         %[cm^2/s]
    D2_list = [12*D3, 8*D3, 3*D3];          %[cm^2/s]

    D1 = D1_list(2);                        %[cm^2/s]
    D2 = D2_list(2);                        %[cm^2/s]
    D_avg = (D1*L_1 + D3*(L_f - L_1))/L_f;  %[cm^2/s]

    k = 2.77*10^-7;                         %[mg/s]
    k_avg = k*(L_f - L_1)/L_f;              %[mg/s]


    T = 9*4*7*24*60*60;                     %[s]

    Cs_list = [0.7, 1.5, 1.8];              %[mg/cm^3]
    color = ['r','g','b','k'];              %[mg/cm^3]


    dx = L_f/100;
    dt = T/90;
    xmesh = 0: dx: L_f;
    tmesh = 0: dt: T;
    nx = length(xmesh);
    nt = length(tmesh);



%% 1 section model: analytical soln

    sol_anal = zeros(nx, nt);
    Cs = Cs_list(2);
    D1 = D1_list(2);
    D2 = D2_list(2);


    An = @(n) (4*Cs/(pi*(2*n + 1))) * sin(pi*((1/2) + n)*(L_1/L_f));
    sqrl = @(n) (pi/L_f) * ((1/2) + n);
    for n = 0:500
        for x = 1:nx
            for t = 1:nt
                sol_anal(x, t) = sol_anal(x, t) ...
                    + An(n)*cos(sqrl(n)*xmesh(x))...
                    *exp(-(sqrl(n)^2 + k_avg/D_avg)*D_avg*tmesh(t));
            end
        end
    end


    figure()
```

```matlab
    plot(xmesh, sol_anal(:,1)');
    title('IC with analytical solution')
    xlabel('x [cm]')
    ylabel('C(x, 0) [mg/cm^3] ')


    figure()
    surf(xmesh, tmesh/(60*60*24*7*4), sol_anal');
    title(['Analytical solution when Cs = ',num2str(Cs),'mg/cm^3'])
    xlabel('x [cm]')
    ylabel('t [month]')
    zlabel('C(x,t) [mg/cm^3]')


    figure()
    for i = 1:length(Cs_list)
        Cs = Cs_list(i);
        for n = 0:500
            for x = 1:nx
                for t = 1:nt
                    sol_anal(x, t) = sol_anal(x, t) ...
                        + An(n)*cos(sqrl(n)*xmesh(x))...
                        *exp(-(sqrl(n)^2 + k_avg/D_avg )*D_avg*tmesh(t));
                end
            end
        end

        plot(xmesh, sol_anal(:,end), color(i))
        title(['Analytical solution. When t = ',...
            num2str(tmesh(end)/(60*60*24*7*4)),'months'])
        xlabel('x [cm]')
        ylabel('C(x)[mg/cm^3]')
        hold on
    end
    hold off
    legend(['Cs = ', num2str(Cs_list(1)),'mg/cm^3'],...
        ['Cs = ',num2str(Cs_list(2)),'mg/cm^3'],...
        ['Cs = ',num2str(Cs_list(3)),'mg/cm^3']);




    %% 1 section model: numerical solution

    Cs = Cs_list(2);
    D1 = D1_list(2);
    D2 = D2_list(2);



    u_pdepe1 = pdepe(0, @pdefun1, @ic, @bc, xmesh, tmesh);


    figure()
    plot(xmesh, u_pdepe1(1,:));
    title('IC using MATLAB''s pdepe: 1 layer')
    xlabel('x [cm]')
    ylabel('C(x,0) [mg/cm^3]')
```

```matlab
    figure()
    surf(xmesh, tmesh/(60*60*24*7*4), u_pdepe1);
    title(['Using Matlab''s pdepe: 1 layer. Cs = ',num2str(Cs), 'mg/cm^3'])
    xlabel('x [cm]')
    ylabel('t [month]')
    zlabel('C(x,t) [mg/cm^3]')

    figure()
    for i = 1:length(Cs_list)
        Cs = Cs_list(i);
        u_pdepe1 = pdepe(0, @pdefun1, @ic, @bc, xmesh, tmesh);
        plot(xmesh, u_pdepe1(end,:), color(i))
        title(['1 layer. When t = ',num2str(tmesh(end)/(60*60*24*7*4)),'
months'])
        xlabel('x [cm]')
        ylabel('C(x) [mg/cm^3]')
        hold on
    end
    hold off
    legend(['Cs = ', num2str(Cs_list(1)),'mg/cm^3'],...
        ['Cs = ',num2str(Cs_list(2)),'mg/cm^3'],...
        ['Cs = ',num2str(Cs_list(3)),'mg/cm^3']);

    %% 2 section model: numerical solution

    Cs = Cs_list(2);
    D1 = D1_list(2);
    D2 = D2_list(2);


    u_pdepe2 = pdepe(0, @pdefun2, @ic, @bc, xmesh, tmesh);

    figure()
    plot(xmesh, u_pdepe2(1,:));
    title('IC using Matlab''s pdepe: 2 layers')
    xlabel('x [cm]')
    ylabel('C(x,0) [mg/cm^3]')


    figure()
    surf(xmesh, tmesh/(60*60*24*7*4), u_pdepe2);
    title(['Using Matlab''s pdepe: 2 layers. Cs = ',num2str(Cs), ...
        'mg/cm^3, D1 = ',num2str(D1),'cm^2/s'])
    format shortE
    xlabel('x [cm]')
    ylabel('t [month]')
    zlabel('C(x,t)[mg/cm^3]')

    figure()
    for i = 1:length(Cs_list)
        Cs = Cs_list(i);
        u_pdepe2 = pdepe(0, @pdefun2, @ic, @bc, xmesh, tmesh);
        plot(xmesh, u_pdepe2(end,:), color(i))
```

```matlab
        title(['2 layers. When t = ',num2str(tmesh(end)/(60*60*24*7*4)),...
            ' months',', D1 = ',num2str(D1),'cm^2/s'])
        xlabel('x [cm]')
        ylabel('C(x) [mg/cm^3]')
        hold on
    end
    hold off
    legend(['Cs = ', num2str(Cs_list(1)),'mg/cm^3'],...
        ['Cs = ',num2str(Cs_list(2)),'mg/cm^3'],...
        ['Cs = ',num2str(Cs_list(3)),'mg/cm^3']);


    figure()
    Cs = Cs_list(2);
    for i = 1:length(D1_list)
        D1 = D1_list(i);
        u_pdepe2 = pdepe(0, @pdefun2, @ic, @bc, xmesh, tmesh);
        plot(xmesh, u_pdepe2(end,:), color(i))
        title(['2 layers. When t = ',num2str(tmesh(end)/(60*60*24*7*4)),...
            ' months',', Cs = ',num2str(Cs),'mg/cm^3'])
        xlabel('x [cm]')
        ylabel('C(x) [mg/cm^3]')
        hold on
    end
    hold off
    legend(['D1 = ', num2str(D1_list(1)),'cm^2/s'],...
        ['D1 = ',num2str(D1_list(2)),'cm^2/s'],...
        ['D1 = ',num2str(D1_list(3)),'cm^2/s']);


    figure()
    Cs = Cs_list(2);
    for i = 1:length(D1_list)
        D1 = D1_list(i);
        u_pdepe2 = pdepe(0, @pdefun2, @ic, @bc, xmesh, tmesh);
        plot(tmesh/(60*60*24*7), u_pdepe2(:,round(nx*8/9)), color(i))
        title(['2 layers. Where x = ',num2str(xmesh(round(nx*8/9))),...
            ' cm',', Cs = ',num2str(Cs),'mg/cm^3'])
        xlabel('t [weeks]')
        ylabel('C(x) [mg/cm^3]')
        hold on
    end
    hold off
    legend(['D1 = ', num2str(D1_list(1)),'cm^2/s'],...
        ['D1 = ',num2str(D1_list(2)),'cm^2/s'],...
        ['D1 = ',num2str(D1_list(3)),'cm^2/s']);

    %% 3 section model: numerical solution

    Cs = Cs_list(2);
    D1 = D1_list(2);
    D2 = D2_list(2);



    u_pdepe3 = pdepe(0, @pdefun3, @ic, @bc, xmesh, tmesh);
```

```matlab
    figure()
    plot(xmesh, u_pdepe3(1,:));
    title('IC using MATLAB''s pdepe: 3 layers')
    xlabel('x [cm]')
    ylabel('C(x,0)[mg/cm^3] ')


    figure()
    surf(xmesh, tmesh/(60*60*24*7*4), u_pdepe3);
    title(['Using MATLAB''s pdepe: 3 layers. Cs = ',num2str(Cs), ...
        'mg/cm^3, D2 = ',num2str(D2),'cm^2/s'])
    xlabel('x [cm]')
    ylabel('t [months] ')
    zlabel('C(x,t)[mg/cm^3]')


    figure()
    for i = 1:length(Cs_list)
        Cs = Cs_list(i);
        u_pdepe3 = pdepe(0, @pdefun3, @ic, @bc, xmesh, tmesh);
        plot(xmesh, u_pdepe3(end,:), color(i))
        title(['3 layers. When t = ',num2str(tmesh(end)/(60*60*24*7*4)),'
months'])
        xlabel('x [cm]')
        ylabel('C(x)[mg/cm^3]')
        hold on
    end
    hold off
    legend(['Cs = ', num2str(Cs_list(1)),'mg/cm^3'],...
        ['Cs = ',num2str(Cs_list(2)),'mg/cm^3'],...
        ['Cs = ',num2str(Cs_list(3)),'mg/cm^3']);


    figure()
    Cs = Cs_list(2);
    for i = 1:length(D1_list)
        D2 = D2_list(i);
        u_pdepe3 = pdepe(0, @pdefun3, @ic, @bc, xmesh, tmesh);
        plot(xmesh, u_pdepe3(end,:), color(i))
        title(['3 layers. When t = ',num2str(tmesh(end)/(60*60*24*7*4)),...
            ' months',', Cs = ',num2str(Cs),'mg/cm^3'])
        xlabel('x [cm]')
        ylabel('C(x)[mg/cm^3]')
        hold on
    end
    hold off
    legend(['D2 = ', num2str(D2_list(1)),'cm^2/s'],...
        ['D2 = ',num2str(D2_list(2)),'cm^2/s'],...
        ['D2 = ',num2str(D2_list(3)),'cm^2/s']);


    figure()
    Cs = Cs_list(2);
    for i = 1:length(D1_list)
        D2 = D2_list(i);
        u_pdepe3 = pdepe(0, @pdefun3, @ic, @bc, xmesh, tmesh);
        plot(tmesh/(60*60*24*7), u_pdepe3(:,round(nx*8/9)), color(i))
        title(['3 layers. Where x = ',num2str(xmesh(round(nx*8/9))),...
            ' cm',', Cs = ',num2str(Cs),'mg/cm^3'])
```

```matlab
        xlabel('t [weeks]')
        ylabel('C(x) [mg/cm^3]')
        hold on
    end
    hold off
    legend(['D2 = ', num2str(D2_list(1)),'cm^2/s'],...
        ['D2 = ',num2str(D2_list(2)),'cm^2/s'],...
        ['D2 = ',num2str(D2_list(3)),'cm^2/s']);



end


%==================================================================
% 1 section model
function [c, f, s] = pdefun1(x, t, u, DuDx)
    global D_avg
    global k_avg

    c = 1;
    f = D_avg * DuDx;
    s = -k_avg * u;
end


% 2 section model
function [c, f, s] = pdefun2(x, t, u, DuDx)
    global L_1
    global D1
    global D3
    global k

    c = 1;

    if x < L_1
        f = D1*DuDx;
        s = 0;
    else
        f = D3*DuDx;
        s = -k*u;
    end
end


% 3 section model
function [c, f, s] = pdefun3(x, t, u, DuDx)
    global L_1
    global L_2
    global D1
    global D2
    global D3
    global k

    c = 1;
```

```matlab
    if x < L_1
        f = D1*DuDx;
        s = 0;
    elseif x < L_2
        f = D2*DuDx;
        s = 0;
    else
        f = D3*DuDx;
        s = -k*u;
    end

end


% Initial condition
function u0 = ic(x)
    global Cs
    global L_1
    u0 = Cs*(x < L_1);
end


% Boundary condition
function [pl, ql, pr, qr] = bc(xl, ul, xr, ur, t)
    pl = 0;
    ql = 1;
    pr = ur;
    qr = 0;
end
```